Earth and Space Science

RESEARCH ARTICLE
10.1029/2018EA000391

Crosstalk Effect and Its Mitigation in Aqua MODIS Middle-Wave Infrared Bands

Junqiang Sun[1,2], **Bruce Guenther**[3,4], **and Menghua Wang**[1]

[1]NOAA National Environmental Satellite, Data, and Information Service Center for Satellite Applications and Research, University Research Ct., College Park, MD, USA, [2]Global Science and Technology, Greenbelt, MD, USA, [3]Stellar Solutions, Chantilly, VA, USA, [4]The Joint Polar Satellite System, NESDIS, Seabrook, MD, USA

Key Points:
- Crosstalk contamination induces strong striping and remarkable radiometric bias in Aqua MWIR bands
- Crosstalk correction algorithm is applied to correct the crosstalk effect in both BB calibration including WUCD and L1B EV products
- The crosstalk correction successfully removes the stripping and the radiometric bias

Correspondence to:
J. Sun,
junqiang.sun@noaa.gov

Citation:
Sun, J., Guenther, B., & Wang, M. (2019). Crosstalk effect and its mitigation in Aqua MODIS middle-wave infrared bands. *Earth and Space Science*, *6*, 698–715. https://doi.org/10.1029/2018EA000391

Received 9 MAR 2018
Accepted 21 MAR 2019
Accepted article online 6 APR 2019
Published online 2 MAY 2019

Abstract The MODerate-resolution Imaging Spectroradiometer (MODIS) has 36 bands, among which 6, bands 20–25, are middle-wave infrared (MWIR) bands, covering a wavelength range from approximately 3.750 to 4.515 μm. Significant crosstalk effect in Aqua MODIS MWIR bands was found prelaunch and confirmed on-orbit early in the mission. In this paper, the crosstalk effect in these bands is carefully investigated and quantitatively characterized using the instrument's scheduled lunar observations. The crosstalk correction algorithm that we have developed in our previous work is applied to all levels including black body calibration and L1B EV retrievals to mitigate the crosstalk effect in the bands. We show significant crosstalk contaminations among all MWIR bands and also show that these bands have significant crosstalk contaminations from the shortwave infrared bands. We demonstrate that the crosstalk effect has significant impact on onboard black body calibration as well as on EV retrievals. For L1B EV retrievals, these crosstalk effects induce significant radiometric bias as well as strong striping. The radiometric bias is larger than 1.8 K for all detectors of the 4.47-μm band (band 24) for typical scene. Aqua MODIS band 24 detector 1 is most strongly impacted by crosstalk and has a bias that may be as large as 10 K. The crosstalk correction successfully mitigates the striping in the EV images and improves the accuracy of the EV retrievals in the MWIR bands.

1. Introduction

The MODerate-resolution Imaging Spectroradiometer (MODIS) on the Aqua satellite, one of the twin instruments, has played a dominating role in the Earth Observing System of National Aeronautics and Space Administration (Barnes & Salomonson, 1993; Guenther et al., 2002). It has flown successfully for more than 15 years since it was launch in May 2002. Just as its earlier predecessor, Terra MODIS, the performance of Aqua MODIS has been mostly satisfactory (Xiong et al., 2007, Xiong et al., 2008; Xiong, Wenny, Wu, & Barnes, 2009; Xiong, Wenny, Wu, & Salomonson, 2009). However, both Terra and Aqua MODIS have shown considerable degradation in performance after they passed their design lifetime of 6 years (Sun et al., 2012; Wenny et al., 2012). Thus, radiometric calibration of these instruments has played a vital role in ensuring that the scientific value of the higher-level products is maintained (Sun et al., 2012; Wenny et al., 2012; Xiong et al., 2015). Just as in Terra MODIS, Aqua MODIS also is impacted by electronic crosstalk, especially for the thermal emissive bands (TEBs, Sun et al., 2016b). MODIS has 14 TEBs covering a spectral region from about 3.7 to 14.4 μm (Barnes & Salomonson, 1993; Guenther et al., 2002; Xiong et al., 2007, 2008, 2010; Xiong, Wenny, Wu, & Barnes, 2009). Each TEB has 10 in-track detectors, and a quadratic approximation for calibration is applied for each detector to relate the background-subtracted instrument response to the at-sensor-aperture radiance. The coefficients of the quadratic form are calibrated using a warm target, the onboard black body (BB), and a cold target, a view of cold space (CS). The BB and CS are known as onboard calibrators (Xiong et al., 2010, 2015; Xiong, Wenny, Wu, & Barnes, 2009; Xiong, Wenny, Wu, & Salomonson, 2009).

Serious electronic crosstalk has been found recently in Terra MODIS long wave infrared (LWIR) photovoltaic (PV) bands, band centers 6.71–9.73 μm (bands 27–30), by Sun et al. (2011), Sun, Xiong, Li, et al. (2014), Sun, Xiong, Madhavan, and Wenny (2014), Sun et al. (2015a, 2015b), and Sun et al. (2016a, 2016b). The LWIR crosstalk was present from near the beginning of the mission and increased with time dramatically after Terra MODIS passed its designed 6-year lifetime on-orbit (Sun et al., 2015a, 2015b; Sun et al., 2016a; Sun, Xiong, Li, et al., 2014). The crosstalk induced strong striping in Earth view (EV) imagery (Sun et al.,

2015a, 2015b; Sun et al., 2016a; Sun, Xiong, Li, et al., 2014) and long-term radiometric drift in the EV brightness temperature (BT, Sun et al., 2015a, 2015b; Sun et al., 2016a; Sun, Xiong, Li, et al., 2014). The long-term drifts were about 6 K downward, 4 K downward, 1.5 K upward, and 2 K upward in the EV BT for bands 27, 28, 29, and 30, respectively (Sun et al., 2015a, 2015b; Sun et al., 2016a; Sun, Xiong, Madhavan, & Wenny, 2014). The crosstalk also induces unexpected anomalous features in the calibration coefficients (Sun et al., 2015a, 2015b; Sun et al., 2016a, 2016b; Sun, Xiong, Li, et al., 2014). A linear model was developed to describe the crosstalk effect, and a methodology using lunar observations (Barnes et al., 2006; Sun et al., 2007) was established to characterize the crosstalk effect and to derive the crosstalk coefficients required in the linear model by Sun et al. (2011), Sun, Xiong, Li, et al. (2014). The model with the crosstalk coefficients derived from lunar observations was applied to the BB calibration and Level-1B (L1B) EV retrievals for the four Terra MODIS LWIR PV bands (Sun et al., 2011; Sun et al., 2015a, 2015b; Sun et al., 2016b; Sun, Xiong, Li, et al., 2014; Sun, Xiong, Madhavan, & Wenny, 2014). The derived crosstalk coefficients from the lunar observations can successfully remove the striping in L1B EV imagery and the long-term drifts in L1B EV BT (Sun et al., 2015a, 2015b; Sun et al., 2016a; Sun, Xiong, Li, et al., 2014; Sun, Xiong, Madhavan, & Wenny, 2014) by using this model. The model also can clearly explain and significantly reduce the anomalous features in the calibration coefficients that were observed for many years (Sun et al., 2011; Sun et al., 2015a, 2015b; Sun et al., 2016a, 2016b; Sun, Xiong, Li, et al., 2014).

Crosstalk contaminations induce serious problems for higher-level science products such as the cloud mask that uses the L1B products of the LWIR PV bands as input due to its strong scene dependence as well as its strengthening impacts with time (https://modis-images.gsfc.nasa.gov/validation_06.html). These problems can be resolved by applying the crosstalk correction to these bands in both BB calibration and L1B EV retrievals (Sun et al., 2016c). The successful crosstalk correction in Terra LWIR PV bands has drawn great attention in science community, resulting in the implementation of the crosstalk correction in official MODIS L1B products (Collection 6.1, the most recent version) for LWIR PV bands (Wilson et al., 2016). The implementation followed the methodology and algorithms developed by Sun et al. (2011) and Sun, Xiong, Li, et al. (2014). However, the Terra MODIS C6.1 processing makes no crosstalk corrections for early mission observations (Wilson et al., 2016) even though such crosstalk effects are apparent in the lunar observations (Sun et al., 2011; Sun et al., 2015a, 2015b; Sun et al., 2016a; Sun, Xiong, Li, et al., 2014). The implementation (Wilson et al., 2016) has other issues as well (Chu & Dodd, 2019). Details of this effect are beyond the scope of this paper.

Significant crosstalk contaminations are also found and characterized in Aqua MODIS LWIR PV bands (Sun et al., 2016b). The crosstalk effect has profound impact on calibration coefficients and is the root cause of unexpected anomalous features such as sudden jumps in calibration that have been observed for more than 10 years. It also induces strong striping in L1B EV imagery and significant errors in L1B EV BT. An Aqua MODIS crosstalk correction can significantly reduce the anomalous features in calibration coefficients, the striping in L1B EV imagery, and the errors in L1B EV BT. These corrections will improve the quality and accuracy of the L1B retrievals and the quality and accuracy of the higher-level science products. Nonnegligible crosstalk effect is identified and characterized for SNPP VIIRS TEBs (Sun et al., 2017). The crosstalk effect may be one of the main root causes for the striping in EV imagery (Liu et al., 2013) and anomalies in EV BT during a BB warm-up cool-down (WUCD) calibration (Ignatov, 2016). The investigation in this aspect is ongoing and beyond the scope of this study.

MODIS has 6 middle-wave infrared (MWIR) bands, band 20–25, and 4 shortwave infrared (SWIR) bands, band 5–7 and 26 (Barnes & Salomonson, 1993; Guenther et al., 2002; Xiong et al., 2008, 2007; Xiong et al., 2010; Xiong, Wenny, Wu, & Barnes, 2009) located on the S/MWIR focal plane assembly. They are shown in Figure 1, where the detectors are numbered in the data production order. This detector order convention will be carried throughout this whole document. The detector numbering convention used in documents from the Sensor Builder and their supplier network has a detector numbering opposite to the convention used here. The center wavelengths of MWIR bands and their basic specifications are listed in Table 1. Serious crosstalk contaminations among these bands were found prelaunch in both Terra and Aqua MODIS instruments. They were confirmed on-orbit and investigated early in the mission using lunar observations (Sun et al., 2001). An early form of the current linear model for crosstalk effect was developed at the time to describe and mitigate the crosstalk contamination (Sun et al., 2001). The mitigation of the crosstalk

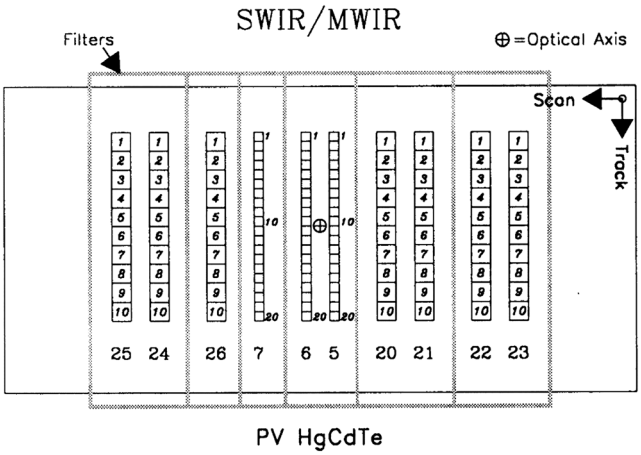

Figure 1. Aqua MODIS SMWIR focal plane assembly. MODIS = MODerate-resolution Imaging Spectroradiometer; MWIR = middle-wave infrared; SWIR = shortwave infrared.

contaminations in these bands was not completely successful due to the complexity of the contaminations considering the involvement of 10 bands and 130 detectors and the lack of understanding of the effect almost two decades ago (Sun et al., 2001).

The current crosstalk model to account for the crosstalk effect (Sun et al., 2011; Sun, Xiong, Li, et al., 2014) is an improved version compared to the model applied early in the mission (Sun et al., 2001) and can be applied to successfully correct the crosstalk contaminations in Aqua MODIS MWIR bands. The crosstalk effect impacts observations for all detectors of the MWIR bands and induces both striping in EV imagery and radiometric bias in EV retrievals. Sun and Wang (2017) have shown that the radiometric bias due to the crosstalk effect can be as large as 10 K for the most impacted detector and 2 K on band average in EV BT retrievals besides the strong crosstalk effect-induced striping in EV imagery in their preliminary analysis. They have also demonstrated that the crosstalk correction can successfully mitigate the crosstalk-induced artifacts in both calibration coefficients and EV retrievals (Sun et al., 2017). The crosstalk effect in MWIR bands also has been investigated by Keller et al. (2017), Keller et al. (2017b), and Keller et al. (2017c) using the methodology developed by Sun et al. (Sun, Xiong, Li, et al., 2014) but in their investigation only crosstalk contamination on detector 1 for each MWIR band and only crosstalk contamination from one detector of one sending band was considered; furthermore, the correction was not applied to BB calibration to correct the crosstalk-induced error in the calibration coefficients of the band. Their analysis was not complete at all levels, including crosstalk effect identification, error in calibration coefficients, and radiometric error in EV retrievals.

In this paper, we will show that there are strong crosstalk contaminations among all Aqua MWIR bands and also with significant crosstalk contaminations from SWIR bands. We will fully characterize the crosstalk effect on a detector basis for all sending band contributions; apply the crosstalk correction in BB calibration in both routine and WUCD; and mitigate the crosstalk impact in EV retrievals and restore quality of the EV imagery and accuracy of the EV retrievals for all Aqua MWIR bands, except Band 21. Band 21 has a much larger dynamic range and consequently has weak responses in typical scenes. The crosstalk correction algorithm will mitigate the crosstalk contaminations in these bands. In section 2, the crosstalk correction methodology and the crosstalk characterization algorithm are reviewed. In section 3, the crosstalk contaminations in MWIR bands are examined and computed based upon the lunar images. Crosstalk coefficients are derived from the scheduled lunar observations. In section 4, the crosstalk correction is applied to the BB calibration to mitigate the crosstalk impact in calibration coefficients derived from BB observations including both WUCD activities and routine operations with BB temperature controlled at 285 K. In section 5, the crosstalk correction is applied to L1B EV retrievals with crosstalk effect corrected calibration coefficients to mitigate the crosstalk contaminations in EV retrievals. Section 6 is a brief summary of this analysis.

Table 1
MODIS Spectral Band Design Specifications

Band	CW (μm)	T_{typ} (K)	Requirement at L_{typ} (%)	Requirement at L_{typ}(K)	Primary use
20	3.75	300	0.75%	0.18	Surface/cloud
21	3.96	335	1%	0.31	temperature
22	3.96	300	1%	0.25	
23	4.05	300	1%	0.25	
24	4.47	250	1%	0.19	Atmospheric
25	4.52	275	1%	0.24	temperature
5	1.24	N/A	2%	N/A	Land/cloud
6	1.64	N/A	2%	N/A	properties
7	2.13	N/A	2%	N/A	
26	1375	N/A	2%	N/A	Cirrus clouds

Note. CW is the center wavelength; T_{typ} is the typical temperature; L_{typ} is the typical radiance. MODIS = MODerate-resolution Imaging Spectroradiometer.

2. Crosstalk Correction Algorithms

Electronic crosstalk is an interfering signal from neighboring detectors on the same focal plane. The extent of the crosstalk is variable and depends on the leaking signal from the sending detectors. A linear model has been developed by Sun et al. (2011, 2001) and Sun, Xiong, Li, et al. (2014) to describe the crosstalk contamination from each sending band, and the overall contribution is assumed to be a linear sum of the crosstalk magnitude from each sending band

$$dn^{\text{xtalk}}_{B_rD_r}(F) = \sum_{B_sD_s} c(B_r, D_r, B_s, D_s) dn^{\text{msr}}_{B_sD_s}(F + \Delta F_{\text{rs}}), \quad (1)$$

where B_r, D_r, B_s, and D_s represent the receiving band, receiving detector, sending band, and sending detector, respectively; $c(B_r, D_r, B_s, D_s)$ is the crosstalk coefficient for the crosstalk contamination from detector D_s of the sending band B_s to detector D_r of the receiving band B_r. F is the pixel number along scan of band B_r, F_{rs} is the frame shift between band B_r and band B_s for viewing the same target. Crosstalk effects occur based on simultaneous observations. The L1B product is produced and published in an Earth-located reference. The detectors in any band are sampled simultaneously with all other detectors in that band, but each band observes the Earth time shifted by the sensor scanning techniques from all other bands on that focal plane. F_{rs} is needed to account for the MODIS scanning technique. $dn^{\text{msr}}_{B_sD_s}$ is the measured background-subtracted instrument response of detector D_s of band B_s, and $dn^{\text{xtalk}}_{B_rD_r}$ is the crosstalk signal from the sending bands to the receiving detector of the receiving band.

Equation (1) can be applied to both TEBs and reflected solar bands (RSBs) (Sun et al., 2001, 2010; Sun, Xiong, Li, et al., 2014). For TEBs, the crosstalk equation can be simplified as (Sun et al., 2011; Sun, Xiong, Li, et al., 2014)

$$dn^{\text{xtalk}}_{B_rD_r}(F) = \sum_{B_s} C(B_r, D_r, B_s) \left\langle dn^{\text{msr}}_{B_sD_s}(F + \Delta F_{\text{rs}}) \right\rangle_{D_s} \quad (2)$$

where $<...>_{\text{D}}$ indicates the average over detectors of a sending band and $C(B_r, D_r, B_s)$ is the effective crosstalk coefficient for the crosstalk contamination from the sending band B_s to detector D_r of the receiving band B_r. Compared to equation (1), the number of crosstalk coefficients in equation (2) is at least reduced by a factor of 10 and a factor of 16 if crosstalk correction applied to MODIS and VIIRS TEBs, respectively. The simplification significantly reduces the complexity of the characterization of the crosstalk effect and computation effort to apply the crosstalk correction to both BB calibration and L1B EV retrievals. We assume that the loss of accuracy with the simplification is small compared to the crosstalk corrections obtained with equation (2). In fact, this approximation has been demonstrated to be valid in our previous investigations and applications (Sun et al., 2011; Sun, Xiong, Li, et al., 2014; Sun, Xiong, Madhavan, & Wenny, 2014; Sun et al., 2015a; Sun et al., 2015b; Sun et al., 2016a, 2016b, 2016c; Sun & Wang, 2016). For Aqua MWIR bands, the loss of accuracy due to the approximation is negligible and within the uncertainty of the TEB calibration as will be demonstrated later in section 5. The crosstalk effect on a receiving detector from a sending detector is taken to be linear and can be either positive or negative with signal on the sending detector.

The crosstalk contaminations can be mitigated by subtracting $dn^{\text{xtalk}}_{B_rD_r}$ from the measured instrument response of the receiving band in both BB and EV measurements (Sun et al., 2011, Sun, Xiong, Li, et al., 2014). The optimal method to determine the crosstalk coefficients is in scenes where the signal onto the receiving detector is 0 and the sender detectors are illuminated. In addition, lunar edges work very well for this purpose. To derive $c(B_r, D_r, B_s, D_s)$, one can directly use the three-dimensional lunar images by assuming that the unexpected signals at the edges of the lunar images are crosstalk contaminations (Sun et al., 2001). To derive $C(B_r, D_r, B_s)$, one cannot directly use the three-dimensional lunar images since the lunar surface is not uniform (Sun et al., 2011, Sun, Xiong, Li, et al., 2014). However, one can produce a two-dimensional profile that is the summation of the dn over scans for each given frame or sample along scan and use the profile instead of dn in equation (2) to derive the $C(B_r, D_r, B_s)$ (Sun et al., 2011; Sun, Xiong, Li, et al., 2014, See Figure 2).

There are also crosstalk contaminations among the detectors within the receiving band. One can include the intraband crosstalk contribution in equations (1) and (2) as well; however, the intraband crosstalk contaminations in BB calibration and in EV observations are expected to cancel each other and the final impact of this crosstalk effect on the EV retrievals is negligible.

3. Crosstalk Coefficients

The 10 S/MWIR bands are located on the S/MWIR focal plane assembly (FPA) shown in Figure 1, and they are known to have crosstalk contaminations among themselves (Sun et al., 2001; Sun & Wang, 2017). The

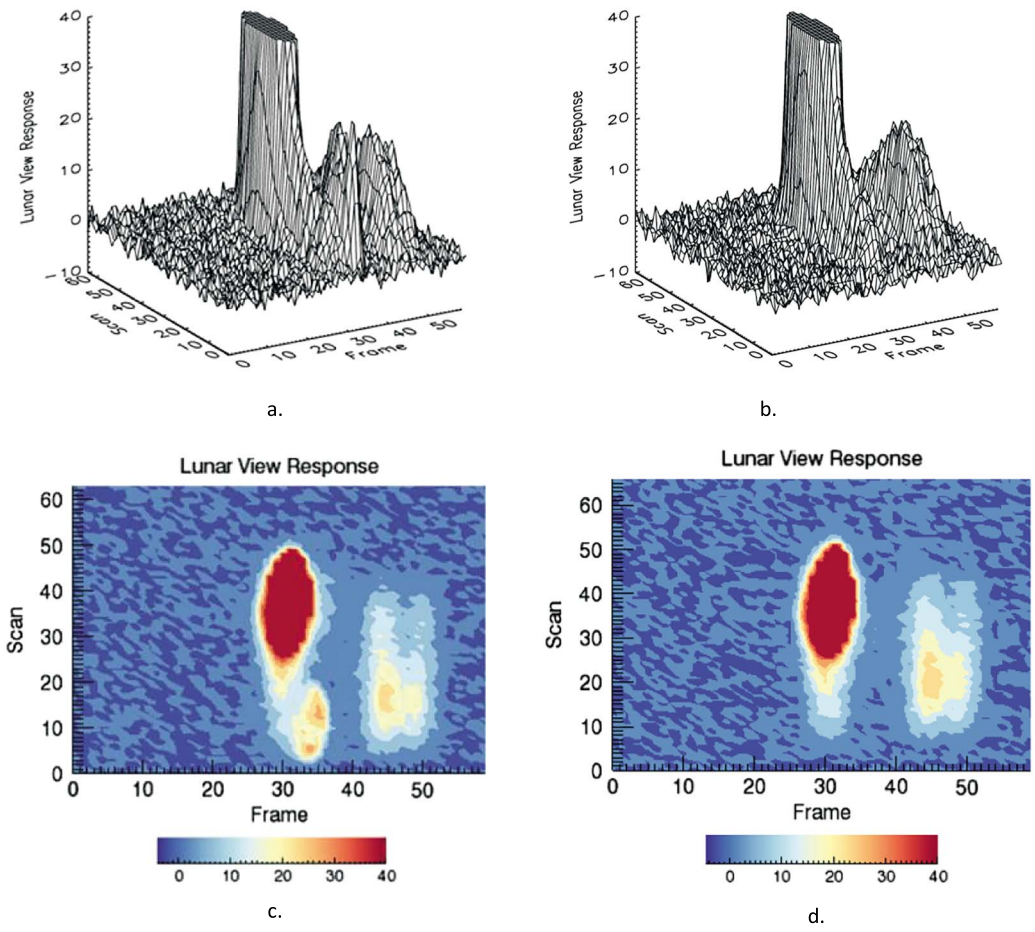

Figure 2. Aqua MODIS band 24 three-dimensional lunar Moon surface images and two-dimensional lunar surface contours: (a) image of detector 1, (b) image of detector 2, (c) contour of detector 1, and (d) contour of detector 2. MODIS = MODerate-resolution Imaging Spectroradiometer.

detectors act both as senders and receivers of crosstalk. Then in principle, each of them can have crosstalk contaminations from nine other bands on the FPA (Sun et al., 2001, Sun & Wang, 2017). The crosstalk contamination from a sending band depends strongly on both the receiving and the sending band. The extent of crosstalk is also very different for each detector of the receiving band. Thus, this poses a huge challenge in identifying the amount of sending signal correctly from each sending band to each detector of a receiving band (Sun et al., 2001, Sun & Wang, 2017). In this analysis, we focus on the crosstalk effect and its mitigation in bands 20–25, all MWIR bands, excluding band 21. Band 21 is a fire application band, whose signal is usually small, needs to be treated differently (Xiong et al., 2008; Xiong, Wenny, Wu, & Barnes, 2009), and its crosstalk contamination and mitigation is beyond the scope of this paper. Even though we focus on the MWIR bands as aforementioned, we consider the contributions of the crosstalk effect from the SWIR bands as well.

The lunar images are the best source to be used to characterize crosstalk effect and derive the crosstalk coefficients (Sun et al., 2011; Sun, Xiong, Li, et al., 2014). Figure 2 shows the lunar images observed by Aqua band 24 detectors 1 and 2 observed on 11 March 2014. The oval cylinders in the centers of the two images are Moon signals, while the neighboring hills and peaks are the crosstalk contaminations. The images are observed by the two detectors in multiple scans, and there is an elongation effect along scan direction in both images due to the so-called oversampling effect (Sun et al., 2007). The figures for the lunar responses are truncated to 40 digital number (dn) to make the crosstalk signals more pronounced. The max lunar responses for band 24 are larger than 4095. In fact, all detectors of band 24 are saturated when they view

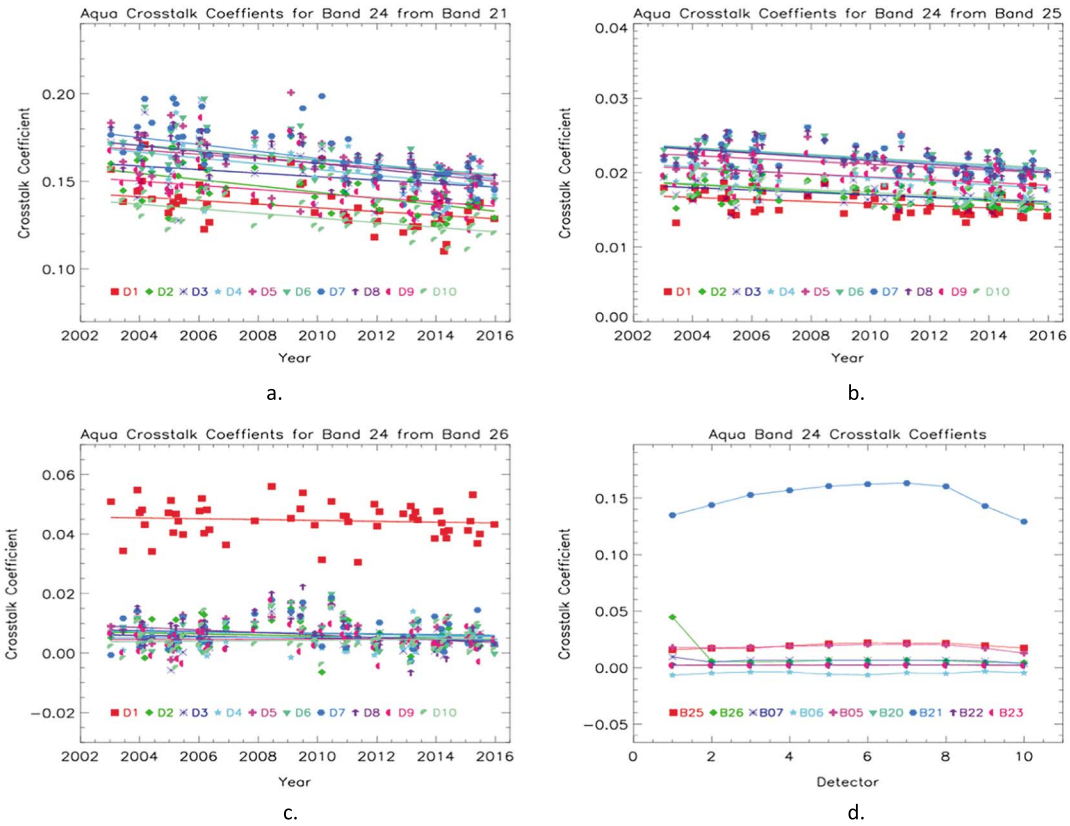

Figure 3. Aqua MODIS band 24 electronic crosstalk coefficients: (a) from band 21, (b) from band 25, (c) from band 26, and (d) time averaged. MODIS = MODerate-resolution Imaging Spectroradiometer.

the center of the Moon. The structure in the right side of the two images is the crosstalk contaminations from bands on the left side of band 24 on the S/MWIR FPA shown in Figure 1. Compared to the lunar image of detector 2, there is an extra peak at the front of the lunar image of detector 1. The peak is mainly the crosstalk contamination from band 26 detector 10. The lunar images of all other detectors are similar to detector 2. Figures 2c and 2d are the contour images of the three-dimensional images in Figures 2a and 2b, from which one can identify the locations of the hill and peaks induced by the crosstalk effect. From their frame shifts from the center of the red oval that is the real lunar image, one can identify the sending bands of the crosstalk contaminations. Similarly one can also identify the sending detectors from their scan shifts from the center of the read oval. Same as seen in Figure 2a, there is an extra peak at the bottom of Figure 2c compared to Figure 2d. The peak is at the spot of the lunar image of band 26 detector 10 if the lunar image of the detector 10 is drawn and, thus, the peak is indeed induced by the contamination of the crosstalk effect.

As stated earlier, one can derive crosstalk coefficients directly using the three-dimensional lunar images (Sun et al., 2001) and one can also derive coefficients using a two-dimensional profile of the lunar observation signals (Sun et al., 2011, Sun, Xiong, Li, et al., 2014). The latter approach reduces the complexity of the derivation and the computational effort when the crosstalk correction applied to both BB calibration and production of the L1B EV retrievals while keeping the accuracy of the correction for TEBs. Thus, in this analysis, we will derive crosstalk coefficients from the lunar profile and apply the crosstalk correction using equation (2). The profile is generated by a simple summation of the lunar signals over scans. The detail for generating the profile and for deriving crosstalk coefficients from the profile can be found in our previous work (Sun et al., 2011, Sun, Xiong, Li, et al., 2014).

Figure 3 shows the crosstalk coefficients that are derived from the lunar observations. Figures 3a–3c display the crosstalk coefficients for all detectors of band 24 for the crosstalk contributions from bands 21, 25, and 26, respectively. The coefficients are strongly dependent on the sending band and are detector dependent,

especially for the crosstalk effect from band 26. The crosstalk contamination from the band 26 to band 24 detector 1 is about five times larger than that to any other detector of the band 24 from band 26. The much larger crosstalk contamination from the band 26 to detector 1 is mainly due to the crosstalk from the band 26 detector 10 as demonstrated in Figure 2 and as discussed previously. The crosstalk coefficients shown in Figures 3a–3c are very stable temporally over the entire mission even though slight decreases with time in the coefficients for the crosstalk contaminations from band 21 are observable. This indicates that the crosstalk effect in Aqua MODIS band 24 does not change much with time. The crosstalk effect in Aqua MODIS band 24 is different from that in MODIS LWIR PV bands, especially in Terra LWIR PV bands, where the crosstalk effect increases with time and sometimes changes dramatically. We take the band 24 crosstalk effect as time independent. Then, we can average the crosstalk coefficients over time and get a set of constant crosstalk coefficients. Band 24 also has crosstalk contaminations from the other 6 sending bands, 5–7, 20, 22, and 23. The crosstalk for the other six sending bands also is found to be stable with time throughout the mission (to the time of the development of this paper), and time-averaged values are also used for these bands in this analysis.

Figure 3d shows the time-averaged crosstalk coefficients for all detectors of band 24 from all 9 sending bands. The crosstalk coefficients for the crosstalk from band 21 are much larger than those from other bands, but since this band has large dynamic range the instrument response to a typical target is at least an order of magnitude smaller compared to those of other MWIR bands. In other words, its actual contribution to the crosstalk contamination of band 24 is about the same as band 25. From Figure 3d, we can see that the crosstalk coefficients for the crosstalk contaminations from bands 20, 22, and 23 are much smaller compared to those of the band 25. The crosstalk coefficients for the contributions from SWIR bands are generally small as well, except for band 5 for all receiving detectors and band 26 for receiving detector 1. Band 24 detector 1 has much larger crosstalk contamination from band 26, mainly from detector 10, compared to other receiving detectors. This results in strong striping in EV imagery, and the stripping will be discussed in more detail later. Figure 3 also clearly demonstrates that removal of the crosstalk contamination from band 26 detector 10 alone is not enough to mitigate the crosstalk impact in band 24. In other words, the investigation done by Keller, Wang, Wu, and Xiong (2017) was not a complete crosstalk effect analysis since only crosstalk contamination from band 26 detector 10 to detector 1 was identified by the authors. Our complete result will be exhibited more clearly in section 5 when the crosstalk correction is applied to EV retrievals.

Figure 4 shows the three-dimensional lunar images observed by detector 1 of Aqua MODIS bands 20–23 and 25, respectively. Again, the center oval cylinders in the lunar images are the Moon view signals truncated to 70, 70, 70, and 120 dn, respectively. The neighboring hills and peaks are the crosstalk contaminations from other S/MWIR bands. Detector 1 of both bands 22 and 25 has a prominent peak in its neighboring area, as is seen also in band 24. The origin of the crosstalk contamination can be identified as band 23 detector 10 and band 24 detector 10 for bands 22 and 25, respectively. For detector 1 of bands 20 and 23, there are two peaks besides the neighboring hills in both of their images. The origins for the peaks can be identified as detectors 1 and 10 of band 23 and detectors 1 and 10 of band 25 for bands 20 and 23, respectively, by looking the contours of the lunar images as has been demonstrated for band 24 in Figures 2c and 2d. No obvious peaks seen in these images are observed in any other detectors, detectors 2–9. Detector 1 and detector 10 crosstalk dependencies of bands likely result from these detectors being preceded/followed by one another in the readout/reset and Analog Signal Processor circuits. Again all detectors in each of the MWIR bands are contaminated by the crosstalk effect from all other MWIR bands even though detector 1 has larger contamination compared to other detectors in the band. It is however not sufficient to only consider the crosstalk effect in detector 1 while limiting crosstalk contamination to only one selected sending detector in one selected sending band as done by Keller, Wang, and Wu (2017b).

The crosstalk coefficients are derived from each individual lunar observation for bands 20, 22, 23, and 25. The coefficients are all independent of time on orbit. We get a single value for the crosstalk coefficients of a given receiving band and detector and a given sending band by averaging the values of the coefficients obtained from individual lunar observations. Figure 5 shows the crosstalk coefficients for bands 20, 22, 23, and 25. For a given MWIR band, the coefficients are about the same for all detectors except detector 1. Detector 1 of each MWIR band has extra crosstalk from detector 10 or from detectors 1 and 10 of a specific sending band as shown in Figure 4 compared to other companions in the same band.

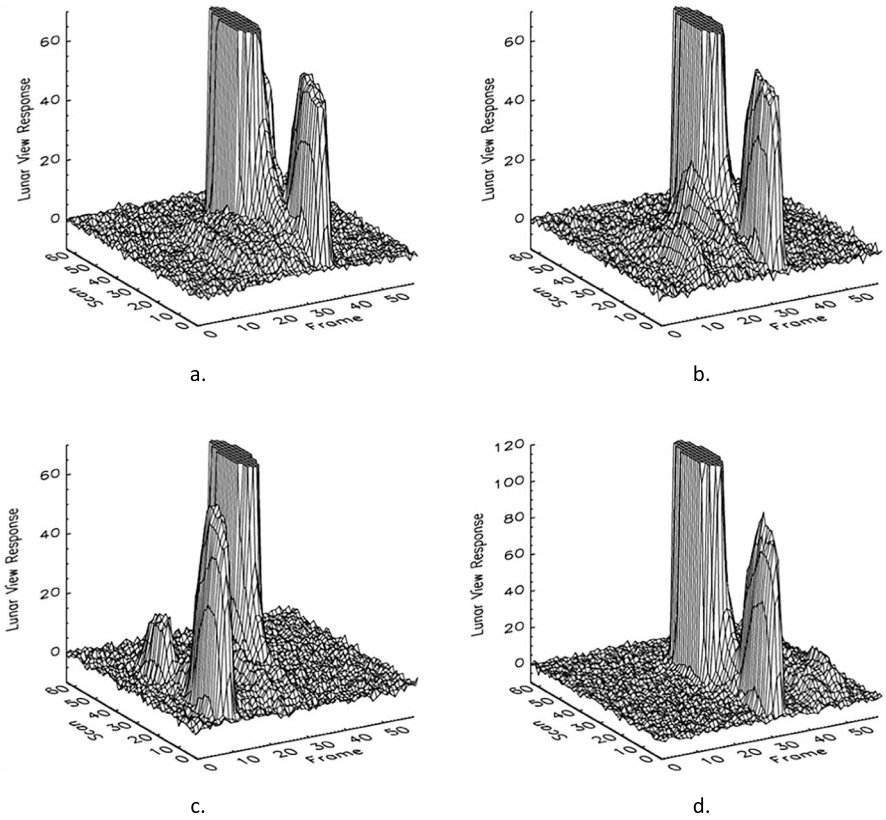

Figure 4. Aqua MODIS MWIR three-dimensional Moon surface images: (a) band 20 detector 1, (b) band 22 detector 1, (c) band 23 detector 1, and (d) band 25 detector 1. MODIS = MODerate-resolution Imaging Spectroradiometer; MWIR = middle-wave infrared.

4. Crosstalk Effect Mitigation in BB Calibration

For MODIS TEBs, a quadratic form is used to approximate the relationship between the "at" sensor radiance L and the background-subtracted instrument response dn

$$L = a_0 + a_1 dn + a_2 dn^2, \tag{3}$$

where a_0, a_1, and a_2 are the offset, linear term, and quadratic term, respectively (Sun et al., 2016b; Xiong et al., 2008; Xiong, Wenny, Wu, & Barnes, 2009; Xiong, Wenny, Wu, & Salomonson, 2009). They are also called calibration coefficients. In equation (3), the unit of the radiance L is Watts/m^2/μm/sr, and dn is the background-subtracted actual response and is unitless. The three calibration coefficients a_0, a_1, and a_2 have the same unit as the radiance. The coefficients, a_0, a_1, and a_2, of the quadratic form may change on-orbit with aging of the instrument. The onboard BB is used to track the changes of the coefficients. A regular scheduled quarterly BB WUCD calibration is performed to update all the coefficients, a_0, a_1, and a_2, while a routine BB calibration with BB temperature controlled at a fixed value is applied to automatically track the change of the linear term during the time period between adjacent WUCD activities, on scan-by-scan basis (Sun et al., 2016b; Xiong et al., 2008; Xiong, Wenny, Wu, & Barnes, 2009; Xiong, Wenny, Wu, & Salomonson, 2009). For Aqua MODIS, the BB is maintained at a nominal operating temperature of 285 K (Xiong et al., 2008; Xiong, Wenny, Wu, & Barnes, 2009; Xiong, Wenny, Wu, & Salomonson, 2009). The linear term is denoted as b1 in the routine BB calibration, to distinguish it from the scheduled BB WUCD calibration.

The background-subtracted instrument response should vanish when the radiance L at sensor approach zero. This requires the offset, a_0, in equation (3) to be zero. In fact, the offset, a_0, has been set to be zero in Aqua MODIS L1B for MWIR bands (Wenny et al., 2012). In this analysis, we set the offset term to zero

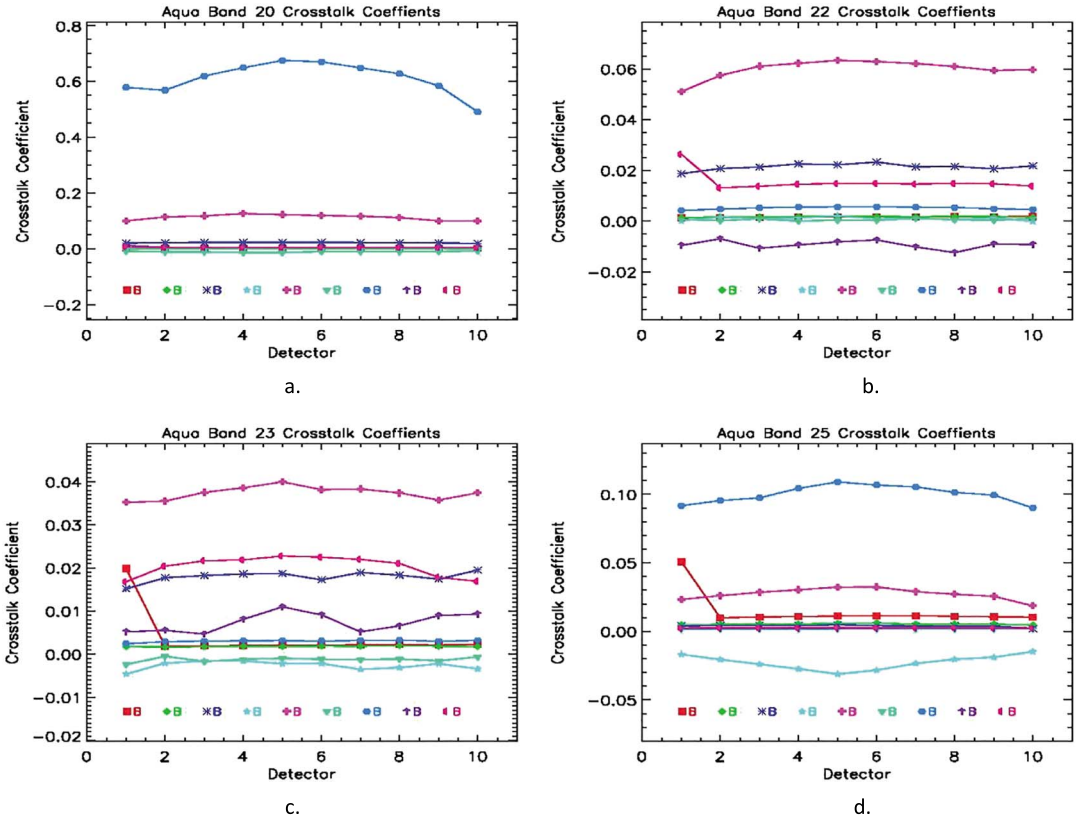

Figure 5. Time-averaged electronic crosstalk coefficients of Aqua MWIR bands: (a) band 20, (b) band 22, (c) band 23, and (d) band 25. MWIR = middle-wave infrared.

when we derive the coefficients of the quadratic form from the WUCD measurements and update the linear term from the routine scan-by-scan BB calibration. Thus, we will focus on a_1 and a_2 in the following analysis and discussions. The detail procedures of the BB WUCD and routine BB calibration can be found in previous works (Sun et al., 2016b; Xiong et al., 2008; Xiong, Wenny, Wu, & Barnes, 2009; Xiong, Wenny, Wu, & Salomonson, 2009). The crosstalk effect in the calibration coefficients can be mitigated by removing the total crosstalk contamination described in either equation (1) or equation (2) from the measured instrument response in both the BB WUCD data as well as the nominal routine scan-by-scan BB measurements.

We have processed the Aqua MODIS BB WUCD data, 57 WUCD events, for entire mission with and without crosstalk correction for MWIR bands and derived the coefficients of the quadratic form for these bands before and after crosstalk correction. There are two sets of data, the BB cool-down data sets and warm-up data sets, each of which can be used to derive the coefficients. Theoretically, the results should be very close for the two sets of data. In current MODIS L1B C6 (https://modis-images.gsfc.nasa.gov/validation_06.html.; Wenny et al., 2012; Sun et al., 2016c), the cool-down data sets are used in the BB WUCD calibration. Hence, for convenience, we only report the results from the cool-down data here and use them in the next section when crosstalk correction is applied to mitigate the crosstalk effect in L1B EV retrievals.

Figure 6 illustrates the derived linear and nonlinear terms, a_1 (b_1) and a_2, for band 24. Figures 6a and 6b display the a_2 before and after crosstalk correction, respectively, for the entire mission. The impacts of the crosstalk effect on the nonlinear terms are clearly visible by comparing the two charts. Figures 6c and 6d show the a_1 (b_1) before and after crosstalk, respectively. The differences between two sets of linear terms are more than 2%. Since the linear term is the dominant coefficient in the quadratic form for all but the warmest observations, a change of 2% in its value implies that the crosstalk effect has a significant impact on the BB calibration of the observations. The a_1 and a_2 terms are computed from BB cycling in quarterly calibrations, and then those values are installed for calibration of observations in equation (3).

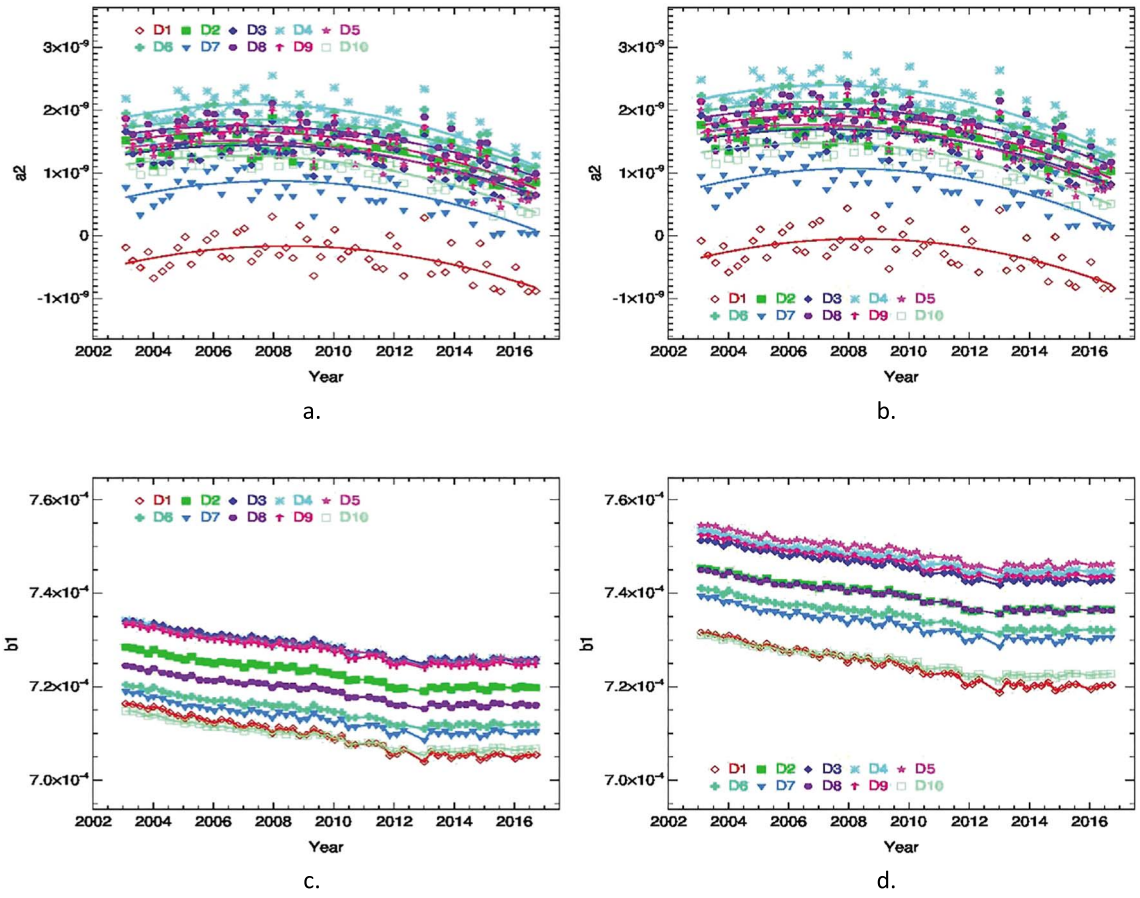

Figure 6. Aqua band 24 calibration coefficients before and after the crosstalk correction for Aqua MODIS band 24: (a) a2 before, (b) a2 after, (c) b1 before, and (d) b1 after. The scales in Figures 6a and 6b, and Figures 6c and 6d are the same to facilitate comparisons of the before and after values. MODIS = MODerate-resolution Imaging Spectroradiometer.

For band 24, there are significant crosstalk contaminations from SWIR bands. Since SWIR bands are RSBs, their background-subtracted instrument responses are zero if there are no crosstalk contaminations from TEBs when they view the BB operating at 285 K. Even if there are crosstalk contaminations from MWIR bands, their instrument responses are small and then their impacts on the MWIR bands due to their electric signals through the crosstalk effect are secondary and negligible in BB calibration. We confirmed this by comparison of Figures 3 and 6. The source in Figure 3 is the Moon, with signal in both the TEB and the RSB. We see large crosstalk effect from band 26, detector 1. In Figure 6, where the source is a thermal signal up to 315 K, with negligible signal in the RSB range, we can see contributions from detector 1 are *in family* with the other detectors (in band 24). Nevertheless, crosstalk contaminations from SWIR bands in EV are significant and play an important role in worsening the quality of Aqua band 24 L1B products at daytime scenes. This topic is investigated in section 5.

The impact of crosstalk effect on the nonlinear terms, a_2, are present for Aqua MODIS bands 20, 22, 23, and 25 (not shown). The crosstalk impact on the linear terms for these bands are much more significant. We focus on the crosstalk impact on the linear terms in following discussion. Figure 7 shows the linear terms, a_1 (b_1) for bands 20 and 22 for the entire mission. For bands 20 and 22, the changes of a_1 are within ~3–4% and ~2–3%, respectively. The changes are significant and consequently the crosstalk effect has serious impact on the two bands. It is noticeable that detector 1 of both bands 20 and 22 has the largest change among all detectors of the same band. As discussed in the previous section and seen in Figure 5, detector 1 of bands 20 and 22 has much larger crosstalk contamination from bands 22 and 23, respectively, comparing to their partners in the same band. Since both bands 22 and 23 are TEBs, detector 1 of both bands has the largest impact among all detector of the same band as expected. Figure 8 represents the linear terms of

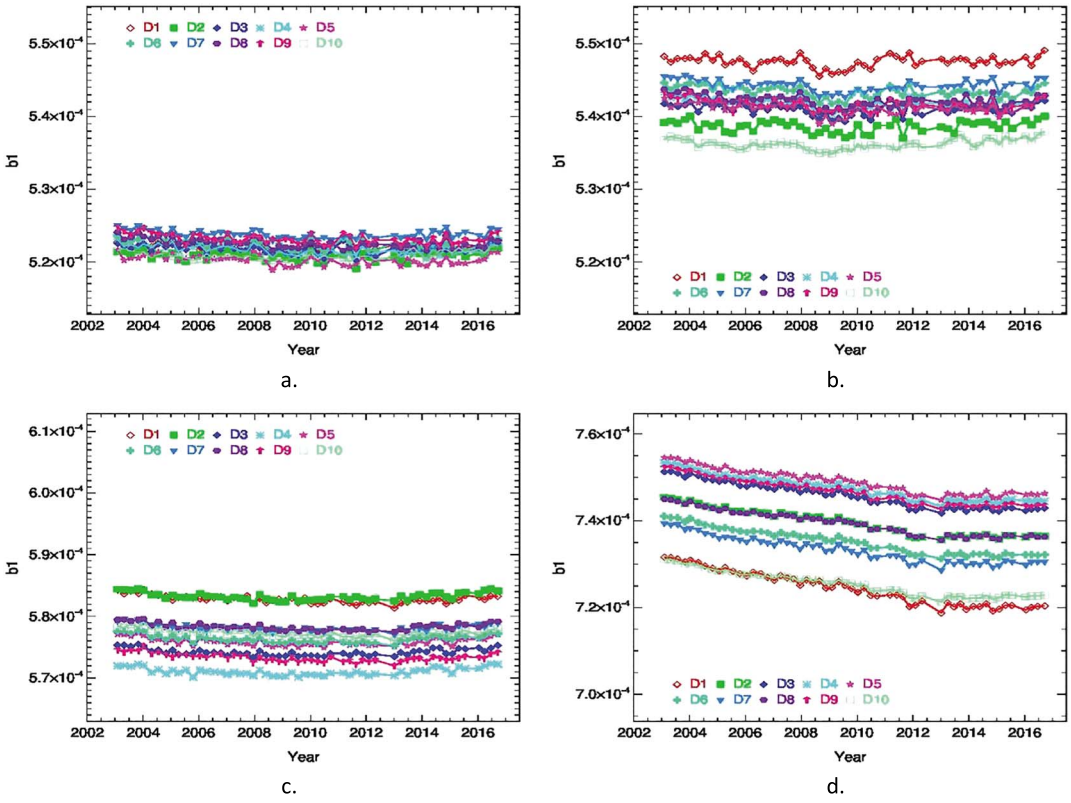

Figure 7. Calibration coefficients before and after the crosstalk correction for Aqua MODIS bands 20 and 22: (a) band 20 b1 before, (b) band 20 b1 (after), (c) band 22 b1 before, and (d) band 22 b1 after. MODIS = MODerate-resolution Imaging Spectroradiometer.

bands 23 and 25 for the entire mission. The changes of the linear terms are about 3% for band 23 and with ~1.2–3% for band 25. The largest change occurs in detector 1 for each of the two bands as expected since detector 1 of the two bands has much larger crosstalk contamination from bands 25 and 24, respectively. Again, crosstalk effects in both of bands 23 and 25 are significant and crosstalk correction should be applied to remove the effect in the two bands as well as in other MWIR bands.

As demonstrated in this section by Figures 6 and 7, crosstalk effect has strong impact in calibration coefficients of Aqua MODIS MWIR bands and one has to remove the effect in the calibration coefficients in order to completely mitigate the crosstalk effect. In the analysis of Keller, Wang, Wu, & Xiong (2017), Keller, Wang, & Wu (2017b), and Keller, Wang, & Wu (2017c), the crosstalk correction was not applied to the BB calibration in addition to the incomplete characterization effort as already pointed out in section 3.

5. Crosstalk Effect Mitigation in L1B EV Retrievals

Crosstalk in L1B EV retrievals for a contaminated band can be mitigated by removing the crosstalk contributions in the EV background-subtracted instrument response and using the crosstalk corrected calibration coefficients including all terms of the quadratic form (Sun et al., 2011; Sun, Xiong, Li, et al., 2014). In this section, we show that the striping in EV imagery of Aqua MODIS MWIR bands also is removal with the crosstalk correction. We also show that the crosstalk effect induces significant radiometric bias in the EV retrievals, and it is necessary to apply the crosstalk correction to eliminate the bias and obtain accurate EV retrievals.

Figure 9 shows typical scene retrieval over Baja Peninsula for Aqua MODIS band 24. The figure is broken into two parts, before and after the crosstalk correction. Figure 9a is the current MODIS C6 (Wenny et al., 2012) retrieved BT over the region. C6 does not apply a crosstalk correction. The data are part of the area covered in the 5-min granule, 2016097.2140, from 6 April 2016 at 21:40:00 to 6 April 2016 at 21:45:00. Strong striping is present in the image. Figure 9b is the histogram of the L1B C6 BT for the various

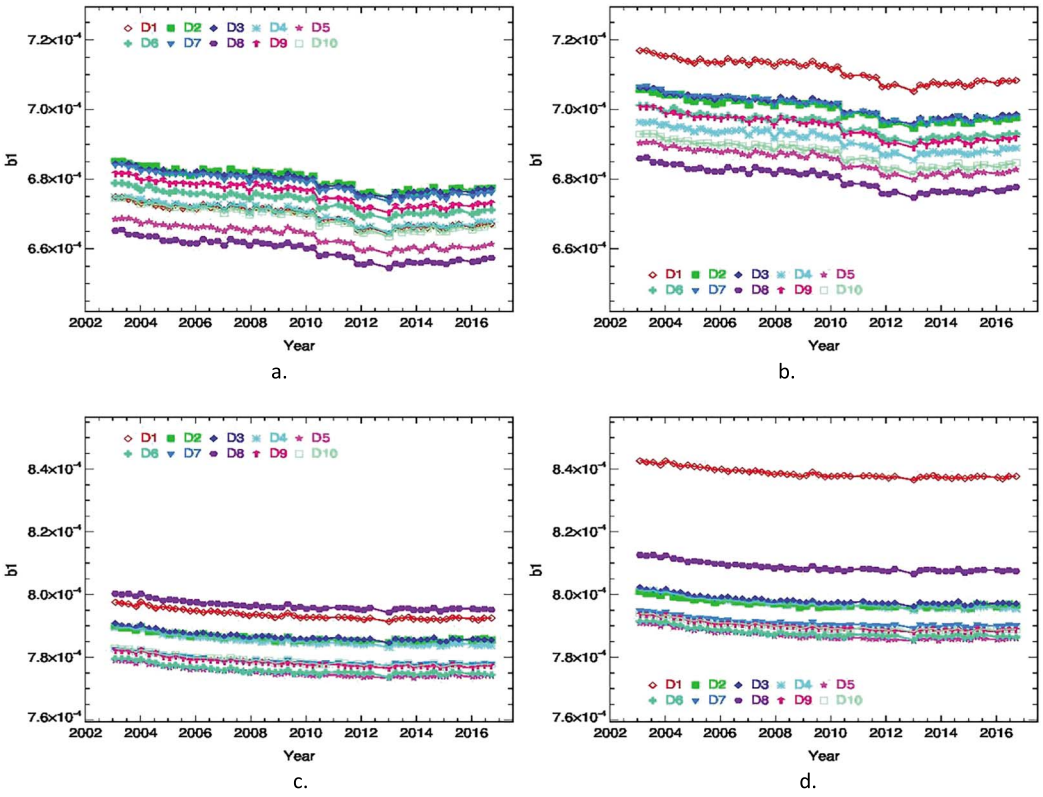

Figure 8. Calibration coefficients before and after the crosstalk correction for Aqua MODIS bands 23 and 25: (a) band 23 b1 before, (b) band 23 b1 (after), (c) band 25 b1 before, and (d) band 25 b1 after. MODIS = MODerate-resolution Imaging Spectroradiometer.

detectors for the whole granule. It is obvious that detector 1 is out of family, especially in cold area, where the bias of detector 1 can be as large as 10 K. Figure 9c is the retrieved BT of the same scene in Figure 9a after the crosstalk correction. The striping seen in the image, Figure 9a, without the crosstalk correction is greatly reduced or removed in the image with the crosstalk correction. Figure 9d displays the histogram of the BT for all detectors after the crosstalk correction for the whole granule. We can see that detector 1 is now no longer out of family, which is consistent with removal of the striping in the image displayed in Figure 9c. From Figures 9b and 9d, we can see that the histogram file after the crosstalk correction has clearly shifted the data toward lower temperatures. Two vertical lines are added to Figures 10b and 10d to indicate the locations of the peak values in the two profiles for each histogram. The difference of the temperature values corresponding to the two vertical lines is about 1.8 K. The granule averaged temperature difference is calculated to be about 2 K. Thus, apart from removal of the striping artifact, a 2-K radiometric bias on granule average basis is induced by the crosstalk effect for Aqua MODIS band 24 for this granule. This suggests that the MODIS L1B C6 band 24 BT appears to have about 2 K higher than actual scene BT. Considering the calibration uncertainty specification for band 24 is 0.19 K, a 2-K bias in the typical scene is a significant error. Detector 1 bias also exceeds the overall average granule bias by a large amount.

Figure 10 shows another scene retrieval for Aqua MODIS band 24. Figure 10a is the Aqua MODIS L1B C6 BT retrieval over a region in the Africa desert. This scene is within the 5-min granule 2017305.1340. Figure 10b is the histogram of the L1B C6 BT for the whole granule. Again, strong striping is present in the image and detector 1 is obviously out of family. Figures 10c and 10d are the corresponding image and histogram of Figures 10a and 10b, respectively, after correction. Striping in the corrected image is removed, and detector 1 is now in the family. About a ~2 K radiometric bias is clearly seen by comparing Figure 10 histograms, and this is nearly the same as seen over the Baja Peninsula in Figure 9. Note also that the histograms in Figure 10 d as well as in Figure 9d are not exactly the same for all detectors after the crosstalk correction. The areas observed are not smooth surfaces, including water-land coast lines and other features, and different detectors see different parts of the scenes, resulting in slightly different histogram of the BT retrieval.

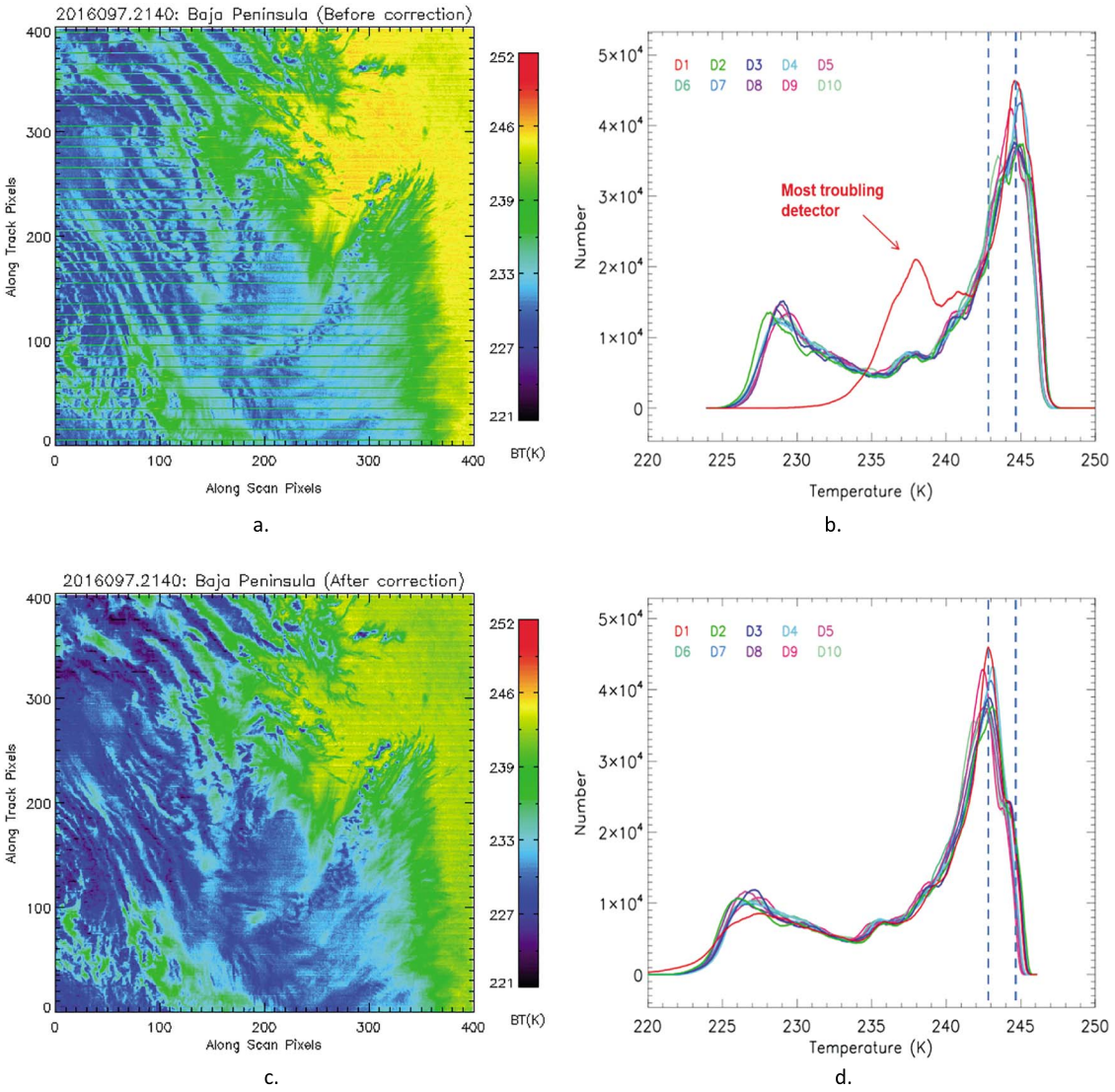

Figure 9. Crosstalk-induced striping and the striping removal in BT of Terra MODIS band 24 at Baja Peninsula in 2016: (a) C6 BT image before crosstalk correction, (b) histogram before crosstalk correction, (c) C6 BT image after crosstalk correction, and (d) histogram after crosstalk correction. BT = brightness temperature; MODIS = MODerate-resolution Imaging Spectroradiometer.

We also have applied the crosstalk correction to the granules of different times and different surface types. Crosstalk effects induce significant striping and radiometric bias in all these granules, and the crosstalk correction successfully mitigates the crosstalk-induced artifacts. The crosstalk contaminations are scene dependent, and the averaged radiometric bias is granule dependent. The granule-averaged radiometric bias for Aqua MODIS band 24 granules already studied varies from 1.8 to 3.3 K. The variation may be even larger for other scenes. It is worth to mention that the large radiometric bias induced by crosstalk effect in MWIR bands was already reported in our previous analysis (Sun, Xiong, Madhavan, & Wenny, 2014). In other literatures (Keller, Wang, & Wu, 2017b; Keller, Wang, & Wu, 2017c; Keller, Wang, Wu, & Xiong, 2017), the radiometric bias was not discovered due to the incompleteness of the analysis as previously mentioned.

Figure 11a is the Aqua MODIS L1B C6 BT retrieval over a region in Africa desert, which is part of the area covered by the 5-min granule 2017306.1240. Striping is seen clearly in the image but with less striping than is evident in Figures 9 and 10. Figure 11b is the histogram of the L1B C6 BT for the whole granule. Detector 1 again is an outlier in this granule even though the situation is much better than that of detector 1 departures

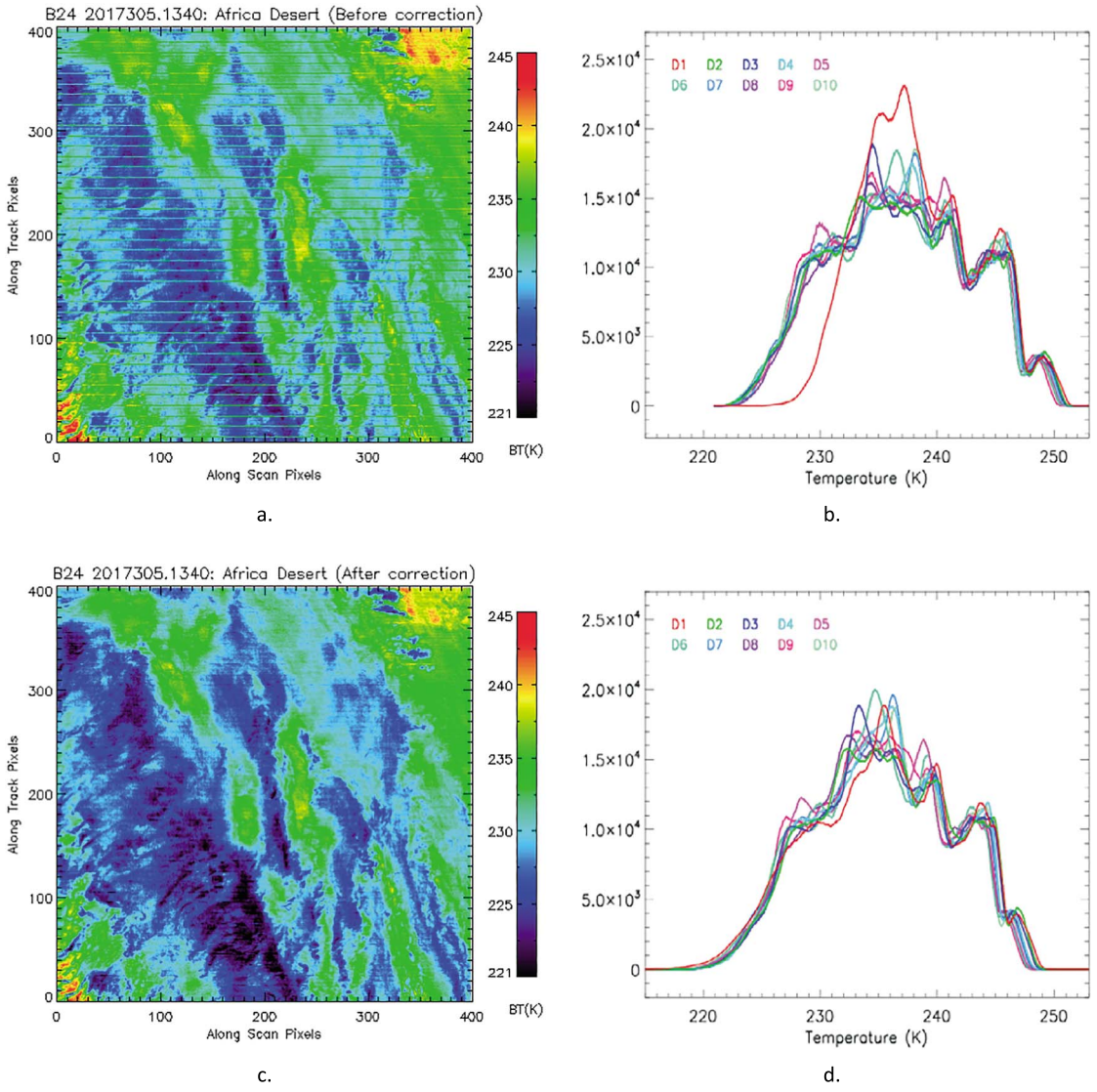

Figure 10. Crosstalk-induced striping and the striping removal in BT of Terra MODIS band 24 at Africa desert in 2016: (a) C6 BT image before crosstalk correction, (b) histogram before crosstalk correction, (c) C6 BT image after crosstalk correction, and (d) histogram after crosstalk correction. BT = brightness temperature; MODIS = MODerate-resolution Imaging Spectroradiometer.

seen in band 24. Figures 11c and 11d are the after correction corresponding image and histogram of Figures 11a and 11b, respectively. The striping seen in Figure 11a is mitigated in the corrected image, and detector 1 returns successfully to in-family after the correction. A small bias of 0.18-K radiometric bias is introduced with the removal of this crosstalk effect. A 0.18-K bias is not necessarily small considering that the uncertainty requirement for band 25 is 0.24 K. The granule-averaged radiometric bias for band 25 also is scene dependent. The granule averaged radiometric bias for band 25 has been found to be as large as 0.26 K in other Earth scenes.

Figure 12 represents a scene retrieval over the Africa desert for Aqua MODIS band 23, the same scene as shown in Figure 11. Figures 12a and 12c are the Aqua MODIS L1B C6 BT retrieval before and after the crosstalk correction, respectively. Again, striping is seen in the image before the correction and striping is removed in the image after the crosstalk correction. Figures 12b and 12d are the histograms for the images before and after the crosstalk correction, respectively. Detector 1 again is out of the family, and the differences between detector 1 and other detectors are about 1 K, similar to what is found in detector 1 in band 25 for this granule. After the crosstalk correction, detector 1 returns in-family as expected. The

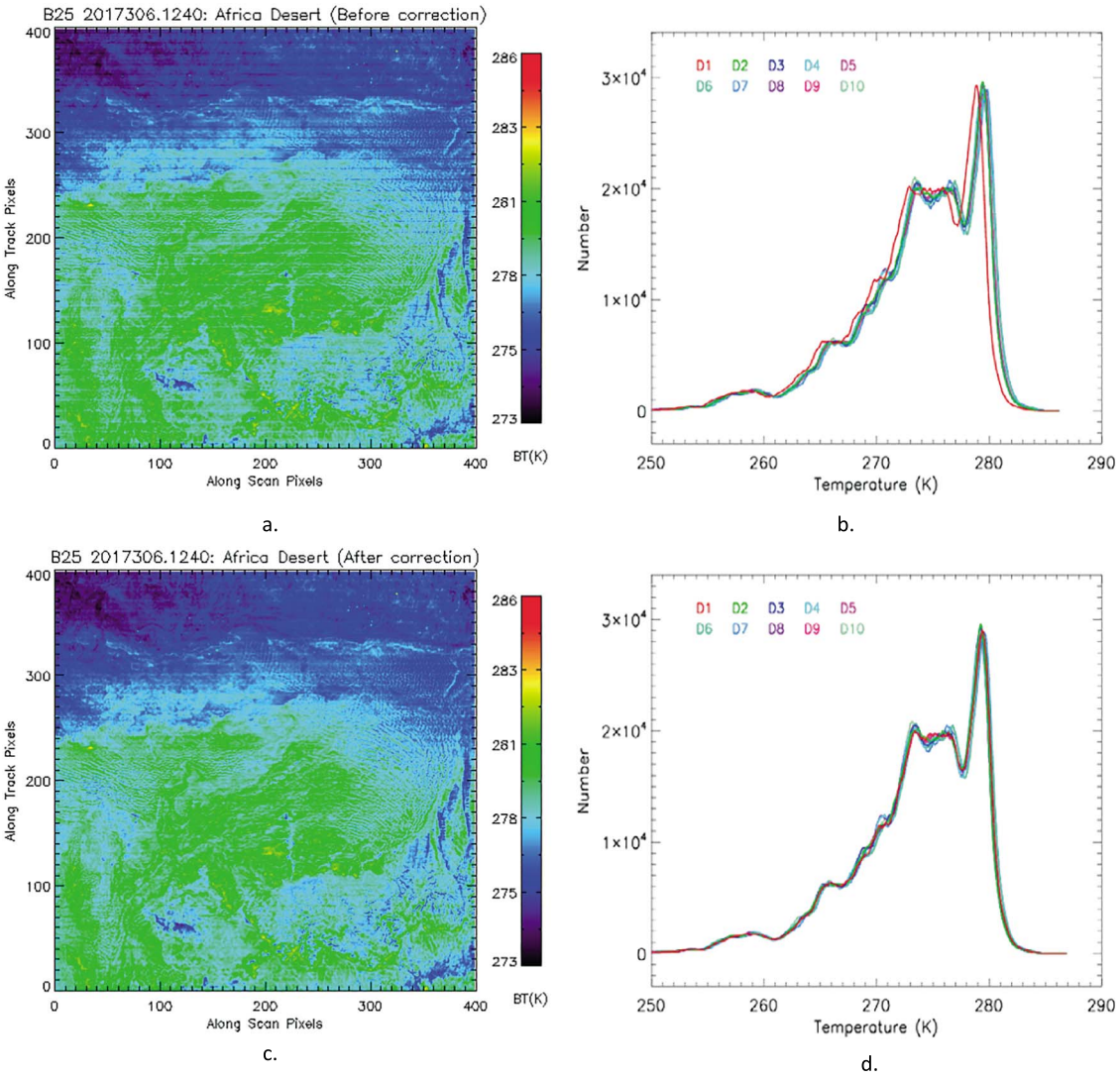

Figure 11. Crosstalk induced striping and the striping removal in BT of Terra MODIS band 25 at Africa desert in 2016: (a) C6 BT image before crosstalk correction, (b) histogram before crosstalk correction, (c) C6 BT image after crosstalk correction, and (d) histogram after crosstalk correction. BT = brightness temperature; MODIS = MODerate-resolution Imaging Spectroradiometer.

granule-averaged radiometric bias in this granule for band 23 is around 0.14 K and is obtained by averaging the differences of the BT retrievals before and after the crosstalk correction. The granule-averaged radiometric bias varies with scene as discussed previously. Larger radiometric bias up to ~0.18 K has been found in other granules. A 0.18-K bias is not necessarily small considering its uncertainty requirement of 0.25 K.

The crosstalk correction also is applied to their L1B C6 EV retrievals for this scene for bands 20 and 22. For these two bands, the striping induced by crosstalk effect is less apparent than in bands 24, 23, and 25. Nevertheless, the quality of the L1B EV imagery for these two bands still is improved with application of the crosstalk correction. The radiometric bias on the basis of granule average varies with scene in bands 20 and 22. The radiometric biases on granule average basis for bands 20 and 22 vary from −0.20 to 0.20 K and from −0.12 to 0.12 K, respectively. Again, the radiometric biases are not negligible considering their uncertainty requirements for bands 20 and 22 are 0.18 and 0.25 K, respectively.

In this section, we demonstrated that the crosstalk effect has significant impact on the L1B EV retrievals of Aqua MODIS MWIR bands. The effect potentially is greatest in band 24. The crosstalk effect both

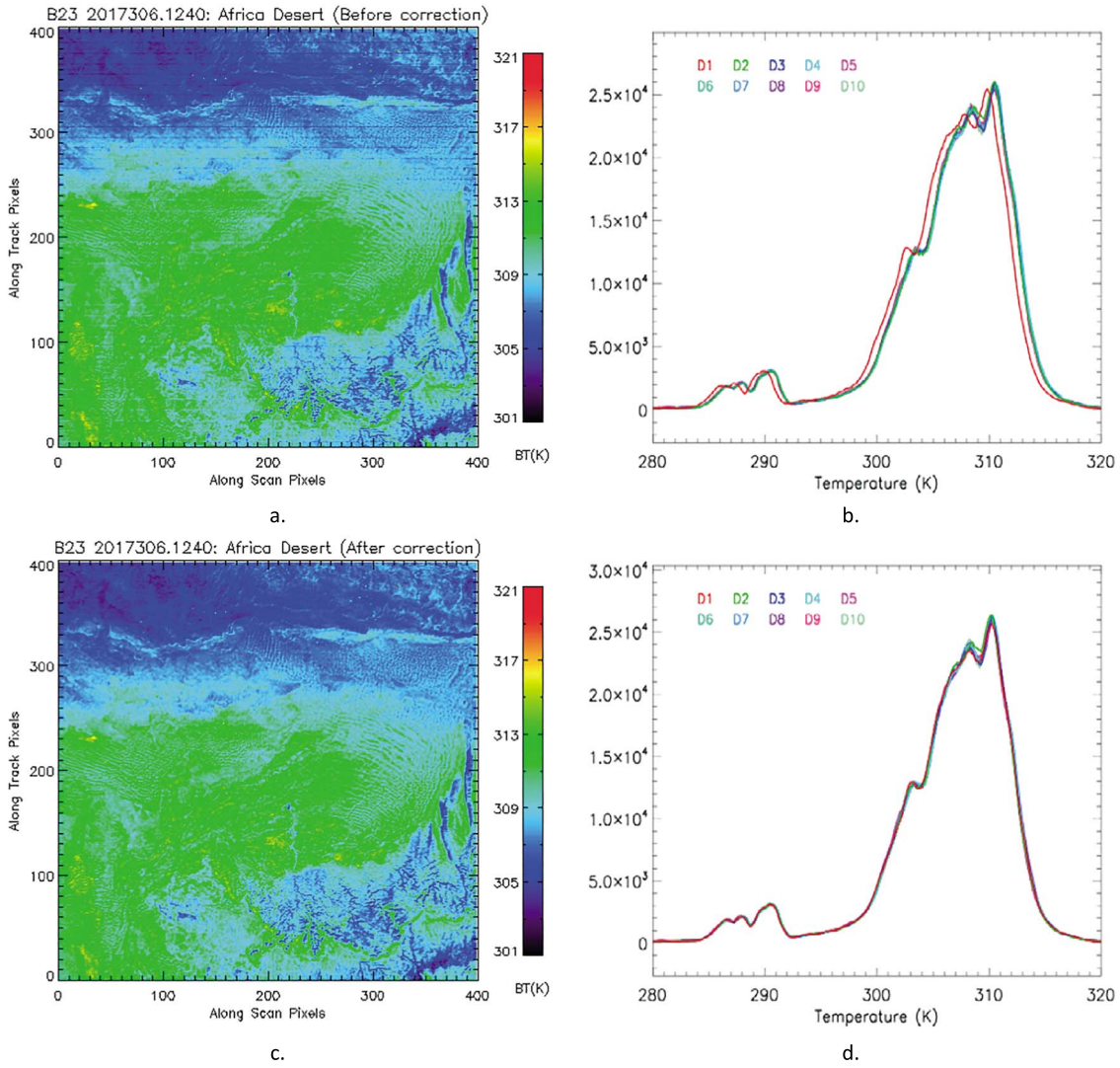

Figure 12. Crosstalk induced striping and the striping removal in BT of Terra MODIS band 23 at Africa desert in 2016: (a) C6 BT image before crosstalk correction, (b) histogram before crosstalk correction, (c) C6 BT image after crosstalk correction, and (d) histogram after crosstalk correction. BT = brightness temperature; MODIS = MODerate-resolution Imaging Spectroradiometer.

deteriorates the quality of the EV imagery and also lessens the accuracy of the EV radiometric retrievals. We showed that the crosstalk correction algorithm (Sun et al., 2011; Sun, Xiong, Li, et al., 2014; Sun, Xiong, Madhavan, & Wenny, 2014) can successfully mitigate the impact of the crosstalk on the EV retrievals and restore both the image quality and the radiometric accuracy of L1B EV retrievals for Aqua MWIR bands. This finding is consistent with our finding for MODIS LWIR bands (Sun et al., 2011; Sun, Xiong, Li, et al., 2014; Sun, Xiong, Madhavan, & Wenny, 2014; Sun et al., 2015a, 2015b; Sun et al., 2016a).

It is also worth to draw attention that the crosstalk effect has significant impact, about a few percent, on the calibration coefficients for all the MWIR bands investigated in this analysis, bands 20 and 22–25, as displayed in Figures 6–8, while the final impact on L1B EV retrievals varies with band. Band 24 has significant impact, bands 23 and 25 have less impact, and bands 20 and 22 have much less impact. In fact, the crosstalk effect in the calibration coefficients derived from the BB calibration and that in EV instrument response has a cancelation effect, resulting in reduction of the crosstalk impact on the final L1V EV retrievals. The cancelation effect depends on the wavelength of the receiving and those of the sending bands. In principle, the closer the wavelengths of the receiving band and a sending band, the larger the cancelation effect.

6. Summary

We fully identified and characterized the crosstalk effect for Aqua MODIS MWIR bands, bands 20, and 22–25, using the routinely scheduled lunar observations. We applied the crosstalk correction to all levels that include WUCD and nominal routine BB calibration, and L1B EV products to mitigate the crosstalk effect in calibration coefficients and L1B EV retrievals. The crosstalk impacts on the linear calibration coefficients (a_1/b_1), the dominant term, are assessed to be about 3–4%, 2–3%, 3%, 3–4%, and 1.2–1.2–3% for bands 20 and 22–25, respectively. By applying the crosstalk correction, the striping artifacts are significantly reduced in the EV imagery. Improved image quality leads us to content that the crosstalk correction also improves the radiometric accuracy of the observations. We also find that the crosstalk effect induces a radiometric bias of 2 K or more in all detectors, in addition to the striping in Aqua MODIS band 24. For detector 1, the bias can be as large as 10 K. The crosstalk effect induces significant radiometric bias in other MWIR bands as well. Thus, the crosstalk correction is necessary for restoring the quality of the EV imagery and the accuracy of EV retrievals for these bands. Since MODIS MWIR bands have applications in surface/atmospheric temperatures, the science products would be greatly improved if the crosstalk correction is applied to official Aqua MODIS L1B for these bands.

Acknowledgments
The MODIS L1A and OBC data used in this analysis are publicly available from NASA's LAADSWEB: https://ladsweb.nascom.nasa.gov/data/, and the MODIS BB WUCD information is available from the MCST's web site: http://mcst.gsfc.nasa.gov/iot/weekly-reports. The views, opinions, and findings contained in this paper are those of the authors and should not be construed as an official NOAA or U.S. Government position, policy, or decision.

References

Barnes, W., & Salomonson, V. (1993). MODIS: A global image spectroradiometer for the Earth observing system, Crit. Rev. Opt. Sci. Technol., CR47, 285–307.

Barnes, W., Xiong, X., Eplee, R. E. Jr., Sun, J., & Lyu, C. (2006). *Use of the Moon for calibration and characterization of MODIS, SeaWiFS, and VIRS, Earth Science Satellite Remote Sensing* (Vol. 2, pp. 98–119). New York: Springer-Verlag.

Chu, M., & Dodd, J. (2019). Examination of Radiometric Deviations in Bands 29, 31, and 32 of MODIS Collection 6.0 and 6.1. *IEEE Transactions on Geoscience and Remote Sensing*. https://doi.org/10.1109/TGRS.2019.2902399

Guenther, B., Xiong, X., Salomonson, V. V., Barnes, W. L., & Young, J. (2002). On-orbit performance of the Earth observing system (EOS) moderate resolution imaging spectroradiometer (MODIS) and the attendant level 1-B data product. *Remote Sensing of Environment*, *83*(1-2), 16–30. https://doi.org/10.1016/S0034-4257(02)00097-4, https://modis-images.gsfc.nasa.gov/validation_06.html

Ignatov, A. JPSS SST STAR progress report. In Proceedings of the STAR 2016 JPSS Annual Science Team Meeting, College Park, MD, USA, 11 August 2016.

Keller, G., Wang, Z., Wu, A., & Xiong, X. (2017). Aqua MODIS band 24 crosstalk striping. *IEEE Geoscience and Remote Sensing Letters*, *14*(4), 475–479. https://doi.org/10.1109/LGRS.2016.2647441

Keller, G. R., Wang, Z., & Wu, A. (2017b). Aqua MODIS electronic crosstalk on SMWIR bands 20 to 26, In Geoscience and Remote Sensing Symposium (IGARSS), 2017, 4174–4177.

Keller, G. R., Wang, Z., & Wu, A. (2017c). Aqua MODIS electronic crosstalk survey from Moon observations. SPIE proc. 10423, 1042314.

Liu, Q., Cao, C., & Weng, F. (2013). Striping in the Suomi NPPVIIRS thermal bands through anisotropic surface reflection. *Journal of Atmospheric and Oceanic Technology*, *30*(10), 2478–2487. https://doi.org/10.1175/JTECH-D-13-00054.1

Sun, J., Angal, A., Xiong, X., Chen, H., Geng, X., Wu, A., et al. (2012). MODIS RSB calibration improvements in Collection 6, Proc. SPIE, 8528, 85280N.

Sun, J., Madhavan, S., & Wang, M. (2016a). Investigation and mitigation of the crosstalk effect in Terra MODIS band 30. *Remote Sensing*, *8*(3), 249. https://doi.org/10.3390/rs8030249

Sun, J., Madhavan, S., & Wang, M. (2016b). Crosstalk effect mitigation in black body warm-up cool-down calibration for Terra MODIS longwave infrared photovoltaic bands. *Journal of Geophysical Research: Atmospheres*, *121*, 8311–8328. https://doi.org/10.1002/2016JD025170

Sun, J., Madhavan, S., & Wang, M. (2016c). Improvement in the cloud mask for Terra MODIS mitigated by electronic crosstalk correction in the 6.7 mm and 8.5 mm channels, *Proc. SPIE*, *9972*, 99720Z.

Sun, J., Madhavan, S., & Wang, M. (2017). Crosstalk effect and its mitigation in Aqua MODIS middle wave infrared bands, *Proc. SPIE*, *10402*, 104020N.

Sun, J., Madhavan, S., Wenny, B., & Xiong, X. (2011). Terra MODIS band 27 electronic crosstalk: Cause, impact, and mitigation, Proceedings of SPIE, 8176, 81760Z.

Sun, J., Madhavan, S., Xiong, X., & Wang, M. (2015a). Investigation of the electronic crosstalk in Terra MODIS band 28. *IEEE Transactions on Geoscience and Remote Sensing*, *53*, 5722–5733.

Sun, J., Madhavan, S., Xiong, X., & Wang, M. (2015b). Long-term trend induced by electronic crosstalk in Terra MODIS band 29. *Journal of Geophysical Research: Atmospheres*, *120*, 9944–9954. https://doi.org/10.1002/2015JD023602

Sun, J., Qiu, S., & Xiong, X. (2001). Electronic crosstalk observed from lunar views and correction with a linear response algorithm, MCST Memo, *M0995*, 1–6.

Sun, J., & Wang, M. (2016). Electronic crosstalk in Aqua MODIS long-wave infrared photovoltaic bands. *Remote Sensing*, *8*(10), 806. https://doi.org/10.3390/rs8100806

Sun, J., & Wang, M. (2017). Crosstalk effect in SNPP VIIRS. *Remote Sensing*, *9*(4), 344. https://doi.org/10.3390/rs9040344

Sun, J., Xiong, X., Barnes, W., & Guenther, B. (2007). MODIS reflective solar bands on-orbit lunar calibration. *IEEE Transactions on Geoscience and Remote Sensing*, *45*(7), 2383–2393. https://doi.org/10.1109/TGRS.2007.896541

Sun, J., Xiong, X., Che, N., & Angal, A. (2010). Terra MODIS band 2 electronic crosstalk: Cause, impact, and mitigation, Proceedings of SPIE, 7826, 78261Y.

Sun, J., Xiong, X., Li, Y., Madhavan, S., Wu, A., & Wenny, B. N. (2014). Evaluation of radiometric improvements with electronic crosstalk correction for Terra MODIS band 27. *IEEE Transactions on Geoscience and Remote Sensing*, *52*, 6497–6507.

Sun, J., Xiong, X., Madhavan, S., & Wenny, B. N. (2014). Terra MODIS band 27 electronic crosstalk effect and its removal. *IEEE Transactions on Geoscience and Remote Sensing*, *52*, 1551–1561.

Wenny, B. N., Wu, A., Madhavan, S., Wang, Z., Li, Y., Chen, N., et al. (2012). MODIS TEB calibration approach in collection 6, Proceedings of SPIE, 8533, 85331M.

Wilson, T., Wu, A., Geng, X., Wang, Z., & Xiong, X. (2016). Analysis of the electronic crosstalk effect in Terra MODIS long-wave infrared photovoltaic bands using lunar images, Proceedings of SPIE, 10004, 100041C.

Xiong, X., Chiang, K., Wu, A., Barnes, W., Guenther, B., & Salomonson, V. (2008). Multiyear on-orbit calibration and performance of Terra MODIS thermal emissive bands. *IEEE Transactions on Geoscience and Remote Sensing*, *46*(6), 1790–1803. https://doi.org/10.1109/TGRS.2008.916217

Xiong, X., Sun, J., Barnes, W., Salomonson, V., Esposito, J., Erives, H., & Guenther, B. (2007). Multiyear on-orbit calibration and performance of Terra MODIS reflective solar bands. *IEEE Transactions on Geoscience and Remote Sensing*, *45*(4), 879–889. https://doi.org/10.1109/TGRS.2006.890567

Xiong, X., Sun, J., Xie, X., Barnes, W., & Salomonson, V. (2010). On-orbit calibration and performance of Aqua MODIS reflective solar bands. *IEEE Transactions on Geoscience and Remote Sensing*, *48*(1), 535–546. https://doi.org/10.1109/TGRS.2009.2024307

Xiong, X., Wenny, B., Wu, A., & Barnes, W. (2009). MODIS on-board blackbody function and performance. *IEEE Transactions on Geoscience and Remote Sensing*, *47*(12), 4210–4222. https://doi.org/10.1109/TGRS.2009.2023317

Xiong, X., Wenny, B., Wu, A., & Salomonson, V. (2009). Aqua MODIS thermal emissive bands on-orbit calibration, characterization, and performance. *IEEE Transactions on Geoscience and Remote Sensing*, *47*(3), 803–814. https://doi.org/10.1109/TGRS.2008.2005109

Xiong, X., Wu, A., Wenny, B. N., Madhavan, S., Wang, Z., Li, Y., et al. (2015). Terra and Aqua MODIS thermal emissive bands on-orbit calibration and performance. *IEEE Transactions on Geoscience and Remote Sensing*, *53*(10), 5709–5721. https://doi.org/10.1109/TGRS.2015.2428198